Accepted Manuscript

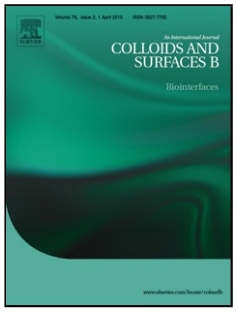

Title: Polyanionic holothurian glycosaminoglycans-doxorubicin nanocomplex as a delivery system for anticancer drugs

Authors: Jiaojiao Mou, Yu Wu, Meijing Bi, Xiaohui Qi, Jie Yang

PII: S0927-7765(18)30242-X
DOI: https://doi.org/10.1016/j.colsurfb.2018.04.032
Reference: COLSUB 9285

To appear in: *Colloids and Surfaces B: Biointerfaces*

Received date: 21-1-2018
Revised date: 8-3-2018
Accepted date: 14-4-2018

Please cite this article as: Jiaojiao Mou, Yu Wu, Meijing Bi, Xiaohui Qi, Jie Yang, Polyanionic holothurian glycosaminoglycans-doxorubicin nanocomplex as a delivery system for anticancer drugs, Colloids and Surfaces B: Biointerfaces https://doi.org/10.1016/j.colsurfb.2018.04.032

Polyanionic holothurian glycosaminoglycans-doxorubicin nanocomplex as a delivery system for anticancer drugs

Jiaojiao Mou[1], Yu Wu[1], Meijing Bi, Xiaohui Qi[2*], Jie Yang[2*]

Weifang Medical University, Weifang 261053, China.

[1] Jiaojiao Mou and Yu Wu contributed equally to this work.

[2] Corresponding authors: Jie Yang, yangjie@wfmc.edu.cn; Co-corresponding authors:Xiaohui Qi, xhjuly0707@163.com.

Graphical Abstract

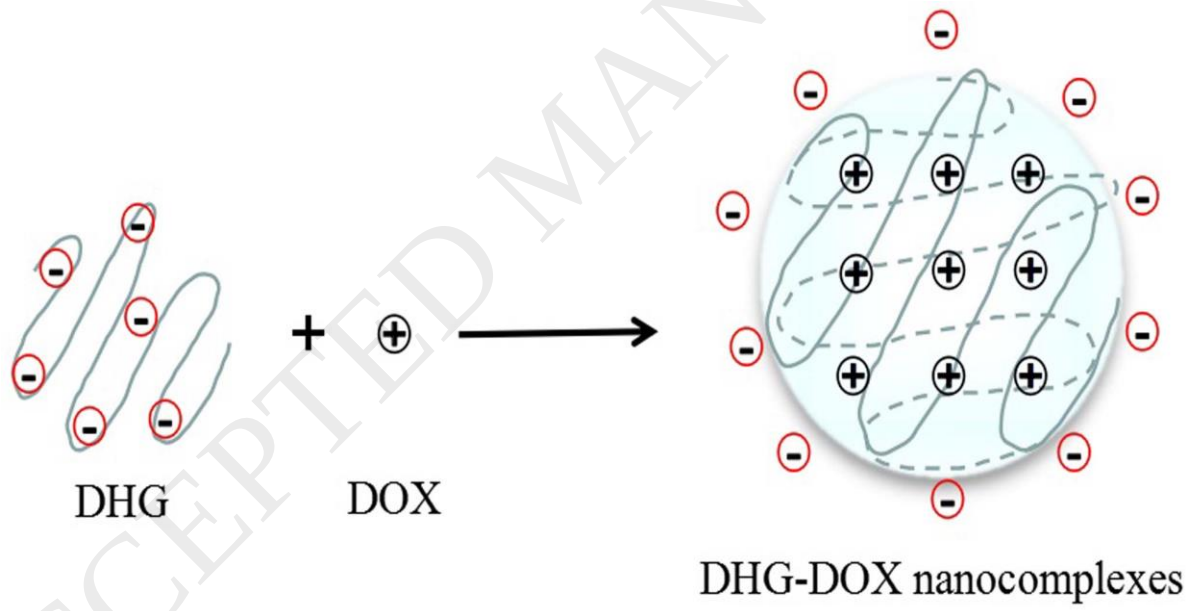

Highlights

- Nanocomplexes was formed by DOX with depolymerized holothurian glycosaminoglycans.
- DHG and DOX formed spherical and smooth nanocomplexes with negative zeta potential.
- The nanocomplexes improved the cytotoxicity of DOX for tumor cells.

Abstract

A nanoscale delivery system for the anticancer drug doxorubicin (DOX) by complexation with depolymerized polyanionic holothurian glycosaminoglycans (DHG) was designed in the present studies. The physicochemical properties of the nanocomplexes were investigated by dynamic light scattering, transmission electron microscopy and zeta potential determination. DHG-DOX interaction was investigated in the presence of ethanol as a hydrogen-bond disrupting agent and NaCl as an electrostatic shielding agent. The thermal properties of nanocomplexes were ascertained by thermogravimetric analysis (TGA). The in vitro release profile was studied as well. Complexation of DHG and DOX formed spherical and smooth nanocomplexes with negative zeta potential (-46.3 mV) at a DHG/DOX (w/w) ratio of 1.0, where drug encapsulation efficiency was over 60%. The results indicated that the the electrostatic and hydrogen bonds played an important role in DHG-DOX complexation. TGA confirmed that the nanocomplexes involved in the DHG as the as the coat and DOX as the content. The release profile of the nanocomplexes exhibited an initial fast release and an subsequent slow and sustained release. Furthermore, the in vitro cell cytotoxicity assays exhibited that the DOX loaded nanocomplexes could improve the cell killing ability of DOX for HepG-2, MCF-7 and A549 tumor cells and exert a sustained-release efforts in the cells.

Keywords: holothurian glycosaminoglycans; doxorubicin; nanocomplexes; antitumor; drug delivery

1. Introduction

Doxorubicin (DOX) is widely used chemotherapeutic drugs in clinical for the treatment of numerous cancers. Despite of its high efficiency, it exhibited an undesirable bone marrow toxicity and cardiotoxicity (Buzdar, Marcus, Smith, & Blumenschein, 2015; Gibaud, Andreux, Weingarten, Renard, & Couvreur, 1994). Moreover, DOX had generated a drug resistance in tumor cells (Chen, Bathula, Li, &

Huang, 2010). One of the approaches to overcome the drug resistance was nanoscale drug delivery system (Tang et al., 2015). Polyanionic carbohydrate, like sulfated polysaccharides, could form polyelectrolyte with positively charged DOX through electrostatic interactions (Pramod, Shah, & Jayakannan, 2015; Xi, Zhou, & Dai, 2012). For instance, dextran sulfate (DS) was successfully used to encapsulate the DOX and overcome the multi-drug resistance in human cancer cells (Tan, Friedhuber, Dunstan, Choong, & Dass, 2010; Parisa, Fatemeh, Vashegani, Ramin, & Rassoul, 2011).

Natural polysaccharides are ideal materials for the preparation of nanoparticles for drug or protein delivery due to many advantages such as natural abundance, generally low cost and mostly bio-compatibility (Wurm, & Weiss, 2014). The success of DS in overcoming the drug resistance and enhancing the entrance of DOX to the cells brought forward the possibility that the sulfated polysaccharides with significant biological properties could be used to encapsulate DOX (Parisa et al., 2011). On the other hand, the formed nanocomplex could elevate the bioavailability of active polysaccharide and help to exhibit its biological functions. Holothurian glycosaminoglycans (HG), which was composed of a chondroitin sulfate backbone substituted at O-3 position of the β-D-glucuronic acid residues with sulfated fucose branches, was also a highly sulfated polysaccharides isolated from sea cucumbers and had exhibited several biological properties, for instance, antiviral, antithrombotic and immune-regulation activities (Mou, Wang, Li, & Yang, 2017). Especially, HG showed a more favorable effect than unfractionated heparin (UFH) on tumor metastasis and neutrophil recruitment without an undesired bleeding risk, promising it a better alternative for UFH as antitumor drugs (Borsig et al., 2007). However, large molecular HG exerted an undesirable effect of platelet aggregation and would cause variety of problems, e.g., high viscosity and low permeability into cells (Mou, Wang, Li, Qi, & Yang, 2017). Free radical degradation method was used to produce the depolymerized HG (DHG) to overcome those obstacles. However, the potential of polyanionic sulfated polysaccharides from marine resources in the nanoscale drug delivery system was rarely reported.

DHG was a more promising candidate than DS for the carrier of the DOX in the

nanocomplex drug delivery system owing to its higher content of sulfate content and antitumor properties (Liu et al., 2016). It also may promote the bioavailability of DHG and exerted a synergistic effect between DHG and DOX on the tumor cells. Herein, the nanocomplex formed by DHG and DOX (DHG-DOX) was investigated. The physicochemical properties of the nanocomplexes, the interaction of DHG-DOX complexation, the release profile of DOX from complex and its in vitro anticancer properties were further studied in the present research.

2. Materials and methods

2.1 Materials

DHG (average molecular weight of 24755 Da) was prepared by free radical degradation of glycosaminoglycan from sea cucumber *Apostichopus japonicus* as described in our previous report (Yang et al., 2015). DOX (purity > 98%) and 3-(4,5-dimethyl-2-yl)-2,5-diphynyl tetrazolium bromide (MTT) were from Sigma. Chitosan (CS, degree of deacetylation> 95%, viscosity: 100-200 mpa.s) was provided by the associate professor Yuanyuan Gao of Weifang Medical University. All other regents were of analytical grade from Sinopharm Chemical Reagent Co., Ltd. (Shanghai, China).

2.2 Preparation and characterization of DHG-DOX nanocomplexes

DOX•HCl was diluted to 0.1 mg/mL with deionized water, which was mixed an equal volume of different concentration of HG solution in deionized water to final DOX/HG (w/w) ratio of 0.6, 0.8, 1.0, 1.5, 2.0, 3.0 and 4.0. The mixtures were stirred for 60 minutes in the lightproof place. The hydrodynamic mean diameter (mean by number) and zeta potential of DHG-DOX complexes were determined by Zetasizer Nano ZS90 (Malven, UK). The dynamic light scattering (DLS) measurements were carried out at 633 nm with a 90º angle detection at room temperature.

2.3 Detection of encapsulation efficiency

The formed nanocomplexes were precipitated by centrifugation at 14000 rpm (2.2×10^4 g) for 30 min. And, a free drug control was performed to ensure that the free DOX was not precipitated. The content of remaining DOX in supernatant was tested at 480 nm by ultraviolet spectrophotometer. The encapsulation efficiency (EE)

was calculated by the following formula:

Encapsulation efficiency (%) = ($[DOX]_{total}$-$[DOX]_{supernatant}$)/ $[DOX]_{total}$ × 100%

2.4 Detection of morphological characteristics

The morphological characteristics of formed nanocomplex were determined by transmission electron microscopy (TEM, Hitachi HT7700 TEM, Japan). For TEM observation, one drop of properly diluted sample was placed on a copper grid and then air dried before examination. The TEM image was acquired on HT7700 microscope at 120 kV equipped with an energy-dispersive X-ray spectrometer.

2.5 DHG-DOX interaction study

To achieve a better understanding of the interaction between DHG and DOX, the prepared nanocomplex was treated with different amount of ethanol as a hydrogen-bond disrupting agent and NaCl as an electrostatic shielding agent (Parisa et al., 2011). Equal volume of ethanol with different concentration was added to the DHG-DOX nanocomplex solution (DOX: 0.5mg/mL, DHG/DOX: 1.0) and the absorbance of the formed mixture at 480 nm was determined by comparison with the pure DOX in the same ethanol-water cosolvent solution. Furthermore, equal volume of NaCl solution with different concentration was added to the DHG-DOX nanocomplex. And, the absorbance of the mixture at 480 nm was determined as well.

Moreover, the absorbance of DHG-DOX solution at 480 nm was tested in the presence of chitosan (CS) as a positively charged polymer, after CS was added to DHG-DOX solution (DOX: 0.5mg/mL, DHG/DOX: 1.0) to different w/w ratio.

2.6 In vitro DOX release studies

DOX release profiles was determined by using PBS (pH: 7.4) as the release medium. Briefly, 3mL nanocomplex solution (DOX: 0.5mg/mL, DHG/DOX: 1.0) was added into dialysis tubing (Mw cutoff 3500 Da) using phosphate buffer solution (PBS) as a release medium. The nanocomplex was incubated in a shaking water bath at 37 °C. A certain volume of the release medium was withdraw and replaced with the same volume of fresh PBS. The amount of DOX in the release medium was determined by fluorospectro photometer. The excitation wavelength was 470 nm and the spectra were recorded at 562 nm.

The cumulative released DOX% = Total released DOX/initial DOX in nanocmplex formulation × 100.

2.7 Thermal properties analysis

The thermal properties of nanocomplexes were ascertained by thermogravimetric analysis (TGA) using DSC-60 instruments (DSC-60, Shimadzu, Japan). The experiments were used an empty sample as the reference. Power X-ray diffraction data were collected on a Bruck D8 Advance diffractometer (Brucker AXS, Germany) with Bragg-Brentano (θ, 2θ) geometry using Cu Kα radiation. The scan was performed at 25 °C from 10-80° in a scanning speed of 0.1s/step.

2.8 In vitro cell cytotoxicity studies

The cytotoxicity of the DHG-DOX nanocomplexes was investigated on the HepG-2 (human hepatoma), A549 (human lung carcinoma) and MCF-7 (human breast adenocarcinoma) cells, which were acquired from Dr Zhang at Weifang Medical University. The cells were maintained in DMEM (Dulbecco's Modified Eagle Medium) medium supplemented with 10% FBS (fetal bovine serum), 100 μg/mL streptomycin and 100 U/mL penicillin at 37 °C under 5% CO_2. Cells were seeded in 96-well tissue culture plates at a density of 5×10^3 cells per well. After 24h, the culture medium was replaced with 200 μL of medium containing equivalent DOX concentrations of 25 μg/mL. The medium was removed after 2h or 24h treatment and the cells were washed with 100 μL of 0.1 M PBS (pH=7.4). The number of viable cells was determined by MTT colorimetric method. The spectrophotometric absorbance was tested on a microplate reader (Thermo, Massachusetts, USA).

2.9 Statistical analysis

All data were taken in triplicate and expressed as mean±SD. Statistical significance was determined unpaired t-test. $p<0.01$ was considered statistically significant.

3. Results and discussion

3.1 Characterization of DHG-DOX nanocomplex

A schematic illustration of the preparation of DHG-DOX nanocomplexes and their abbreviations are shown in Scheme 1. Particle size of nanocomplex plays an

important role in its biological applications, which would influence the cellular uptake, circulating half-life and bio-distribution (Zhang, Taylor, Wan, & Peng, 2012). The variances in the reactant ratios can obviously affect the particle size of the DHG-DOX nanocomplex. As shown in Table 1, the mean hydrodynamic diameter, poly-dispersity index and zeta potential of nanocomplexes composed of 0.05 mg/mL DOX and DHG of different DHG-DOX ratio were investigated. The results indicated that the particle size of nanocomplexes decreased with the increasing amount of DHG, which allowed the formation of monodispersed and homogeneous spherical of the nanocomplexes.

Moreover, Table 1 showed that the surface of the nanocomplexes possessed negative charge, which increased with the increasing amount of DHG. Highly negative charge could avoid nanocomplexes from agglomeration and enhance its colloid stability. The dispersive nanocomplex tended to repel each other and render the colloid stable. The zeta potential value also revealed that the nanocomplexes were comprised with DHG as the coat and DOX as the content. 3.2 Encapsulation efficiency

As shown in Fig. 1, the encapsulation efficiency of DHG-DOX nanocomoplexes was affected by DOX/DHG (w/w) ratio. And, the DOX complexation increased with the increasing DHG/DOX ratio and reached a peak of 64.2% at a ratio of 1:1, which were used to prepare the nanocomples for the further research. Moreover, the DOX encapsulation efficiency in the nanocomplexes with DOX/HG (w/w) ratio between 0.6 and 4.0 were all above 55%, suggesting that the DHG was effective in improving encapsulation efficiency of DOX.

TEM was used to investigate the morphological and structural features of nanocomplexes. The TEM image (Fig. 2) clearly showed that the formed nanocomolex were in the nanoscale range and in regular smooth and spherical shapes. The sizes observed by DLS were larger than those tested by TEM, which was probably due to the solvation shell bound by the DHG coat onto the surface of the DOX core (Zhang et al., 2017).

3.4 Absorbance and florescence spectrum of DHG-DOX nanocomplexes

The absorbance and the florescence spectrum were determined to investigate the

changes of spectra during the formation of nanocomplexes. As shown in Fig. 3A, the formation of nanocomplexes caused a reduction in the absorbance and a bathochromic shift from 479 nm to 491 nm. The similar experiment phenomena was observed in previous reports (Kitaeva, MelikNubarov, Menger, & Yaroslavov, 2004; Manocha, & Margaritis, 2010). A much drastic reduction was observed in the florescence spectrum (Fig. 3B) but no shift in the emission spectrum, which was reported in the previous article (Parisa et al., 2011).

3.5 Interaction of DHG-DOX nanocomplexes

The hydrogen-bond disrupting agent ethanol and electrostatic shielding agent NaCl were added to investigate the interaction between DHG and DOX. The results (Fig. 4A and 4B) showed that addition of ethanol and NaCl lead to the increase of the absorbance of nanocomplexes at 480 nm, indicating the inhibition of complexation of DHG and DOX. The results was in accordance with the previous article (Kitaeva et al., 2004). Moreover, the absorbance of nanocomplexes was equal to that of free DOX when the ethanol concentration above 60% or NaCl concentration above 0.4 M. Besides, polycationic polysaccharide CS could effect the DHG-DOX interaction. As shown in Fig. 4C, the presence of CS, a positively charged polymers, would lead to a increase of the absorbance of nanocomplexes at 480 nm, which reached up to a maximum at CS/DHG (w/w) of 0.5.

The results indicated that the electrostatic and hydrogen bonds played an important role in DHG-DOX complexation. Na^+ and Cl^- shield electrostatic charge of both DHG and DOX. Along with the increased NaCl concentration, the electrostatic interaction of DHG-DOX was gradually disturbed. Furthermore, addition of the H-bond disturbing ethanol caused the destruction of DHG-DOX nanocomplexes.

The in vitro release of the DOX from DHG-DOX nanocomplexes was determined using a dialysis method with a 3500 Da MWCO in PBS as the release medium (Fig. 5). Initially, approximately 40% of the DOX exhibited a burst release within the first hour, which was due to the release of the free DOX. A following fast release was observed during the next 8 h then a slow and sustaining release curve persisted afterwards. The release of DOX from the nanocomplexes was attributed to

the release of the DOX weakly bound with DHG and strongly entrapped DOX. The in vitro release also proved the stability of the nanocomplexes, which could be employed in designing a drug delivery system for cancer therapy.

3.7 Thermal analysis of DHG-DOX nanocomplexes

The thermodynamics of DHG-DOX interaction was investigated by TGA/DSC analysis at a range of 50-800 °C. From the TGA curve (Fig. 6), the first dramatic mass loss of the sample (41.5%) from 200 to 400 °C was due to the decomposition of the DHG capping on the DHG-DOX nanocomplexes. And, the sudden mass decrease upon heating from 600 to 800 °C might associate with the destruction of the DOX. The results also proved that the composition of the nanocomplexes involved the DHG as the as the coat and DOX as the content.

3.8 Cell cytotoxicity assay

The cytotoxicity of the DOX loaded nanocomplexes was investigated in HepG-2, MCF-7 and A549 cells using MTT methods. Fig. 7 showed the relative viability of the HepG-2, MCF-7 and A549 cells after incubation with free DOX·HCl and drug loaded DHG-DOX nanocomplexes for 6 and 12 h. The results revealed that the DHG was almost no toxic to three different tumor cells. DHG-DOX nanocomplexes exhibited lower inhibition activities after 6 h culture compared with free DOX·HCl, and higher inhibition activities after 12 h culture for HepG-2 and A549 cells ($p< 0.05$). Unambiguous results suggested that the nanocomplexes could promote the entrance of DOX into the tumor cells and exert a sustained-release efforts (Tsai et al., 2011). This results indicated that the DHG-DOX nanocomplexes may serve as a good drug carrier for DOX to the cells. Besides, enhanced inhibition of DOX·HCl loaded nanocomplexes would be advantageous in increasing the dose of DOX·HCl and lowering its toxicity in application. Furthermore, the depolymerized holothurian glycosaminoglycans with significant bioactive properties could be released in the tumor micro-environment and exhibited its antitumor and immune-regulation activities, which may provide a new way to the threat the malignant tumor.

4. Conclusion

In the present studies, the depolymerized holothurian glycosaminoglycans with

potential biological properties was used as a capping agent to design a synergetic drug delivery system with efficient drug encapsulation. The drug encapsulation reached up to maximum of 64.2% at a DHG/DOX (w/w) ratio of 1.0. And, the surface of the nanocomplexes possessed negative charges. Combined with TGA analysis, the results indicated that the nanocomplexes involved the DHG as the as the coat and DOX as the content. The interaction studies revealed that the electrostatic interaction and hydrogen bonding played an important role in the formation of the nanocomplexes. The release profile of the nanocomplexes exhibited an initial fast release and an subsequent slow and sustained release. The cell cytotoxicity assays exhibited that the DOX loaded nanocomplexes could improve the cell killing ability of DOX for HepG-2, A549 and MCF-7 cells at 12 h treatment. Interestingly, the nanocomplexes may exert a sustained-release efforts in the cells, which would be advantageous in increasing the dose of DOX·HCl and lowering its toxicity in application.

Acknowledgments

This research was supported by initiation funds for Natural Science Foundation of Shandong Province (ZR2016DL10, ZR2016HB72), Medicine and Health Science Technology Development Projects of Shandong Province (2016WS0674) and doctors of Weifang Medical University. Special thanks for the great work of Jiaojiao Mou on the tumor cell cytotoxicity assays.

References

Borsig, L., Wang, L., Cavalcante, M. C., Cardilo-Reis, L., Ferreira, P. L., & Mourão, P. A., et al. (2007). Selectin blocking activity of a fucosylated chondroitin sulfate glycosaminoglycan from sea cucumber. effect on tumor metastasis and neutrophil recruitment. Journal of Biological Chemistry, 282(20), 14984-91.

Buzdar, A. U., Marcus, C., Smith, T. L., & Blumenschein, G. R. (2015). Early and delayed clinical cardiotoxicity of doxorubicin. Cancer, 55(12), 2761-2765.

Chen, Y., Bathula, S. R., Li, J., & Huang, L. (2010). Multifunctional nanoparticles delivering small interfering rna and doxorubicin overcome drug resistance in cancer. Journal of Biological Chemistry, 285(29), 22639.

Gibaud, S., Andreux, J. P., Weingarten, C., Renard, M., & Couvreur, P. (1994). Increased bone marrow toxicity of doxorubicin bound to nanoparticles. European Journal of Cancer, 30A(6), 820-6.

Kitaeva, M. V., MelikNubarov, N. S., Menger, F. M., & Yaroslavov, A. A. (2004). Doxorubicin−poly(acrylic acid) complexes: interaction with liposomes. Langmuir the Acs Journal of Surfaces & Colloids, 20(16), 6575-9.

Liu, X., Liu, Y., Hao, J., Zhao, X., Lang, Y., & Fan, F., et al. (2016). In vivo anti-cancer mechanism of low-molecular-weight fucosylated chondroitin sulfate (lfcs) from sea cucumber cucumaria frondosa. Molecules, 21(5), 625.

Manocha, B., & Margaritis, A. (2010). Controlled release of doxorubicin from doxorubicin/-polyglutamic acid ionic complex. Journal of Nanomaterials, 5(13), 9.

Mou, J., Wang, C., Li, Q., Qi, X., & Yang, J. (2017). Preparation and antioxidant properties of low molecular holothurian glycosaminoglycans by H_2O2/ascorbic acid degradation. International Journal of Biological Macromolecules, 107PA, 1339-1347.

Mou, J., Wang, C., Li, W., & Yang, J. (2017). Purification, structural characterization and anticoagulant properties of fucosylated chondroitin sulfate isolated from holothuria mexicana. International Journal of Biological Macromolecules, 98, 208.

Parisa, Y., Fatemeh, A., Vashegani, F. E., Ramin, S., & Rassoul, D. (2011). Polyanionic carbohydrate doxorubicin–dextran nanocomplex as a delivery system for anticancer drugs: in vitro analysis and evaluations. International Journal of Nanomedicine, 6(6), 1487.

Pramod, P. S., Shah, R., & Jayakannan, M. (2015). Dual stimuli polysaccharide nanovesicles for conjugated and physically loaded doxorubicin delivery in breast cancer cells. Nanoscale, 7(15), 6636-52.

Tan, M. L., Friedhuber, A. M., Dunstan, D. E., Choong, P. F. M., & Dass, C. R. (2010). The performance of doxorubicin encapsulated in chitosan–dextran sulphate microparticles in an osteosarcoma model. Biomaterials, 31(3), 541-551.

Tang, L., Tong, R., Coyle, V. J., Yin, Q., Pondenis, H., & Borst, L. B., et al. (2015). Targeting tumor vasculature with aptamer-functionalized doxorubicin-polylactide nanoconjugates for enhanced cancer therapy. Acs Nano, 9(5), 5072.

Tsai, H. Y., Chiu, C. C., Lin, P. C., Chen, S. H., Huang, S. J., & Wang, L. F. (2011). Antitumor efficacy of doxorubicin released from crosslinked nanoparticulate chondroitin sulfate/chitosan polyelectrolyte complexes. Macromolecular Bioscience, 11(5), 680–688.

Wurm, F. R., & Weiss, C. K. (2014). Nanoparticles from renewable polymers. Frontiers in Chemistry, 2(2), 49.

Xi, J., Zhou, L., & Dai, H. (2012). Drug-loaded chondroitin sulfate-based nanogels: preparation and characterization. Colloids & Surfaces B Biointerfaces, 100(12), 107-115.

Yang, J., Wang, Y., Jiang, T., Lv, L., Zhang, B., & Lv, Z. (2015). Depolymerized glycosaminoglycan and its anticoagulant activities from sea cucumber apostichopus japonicus. International Journal of Biological Macromolecules, 72, 699-705.

Zhang, J., Taylor, E. W., Wan, X., & Peng, D. (2012). Impact of heat treatment on size, structure, and bioactivity of elemental selenium nanoparticles. International Journal of Nanomedicine, 7(2), 815-825.

Zhang, W., Zhang, J., Ding, D., Zhang, L., Muehlmann, L. A., & Deng, S. E., et al. (2017). Synthesis and antioxidant properties of lycium barbarum polysaccharides capped selenium nanoparticles using tea extract. Artificial Cells Nanomedicine & Biotechnology, 1-8.

Figures captions

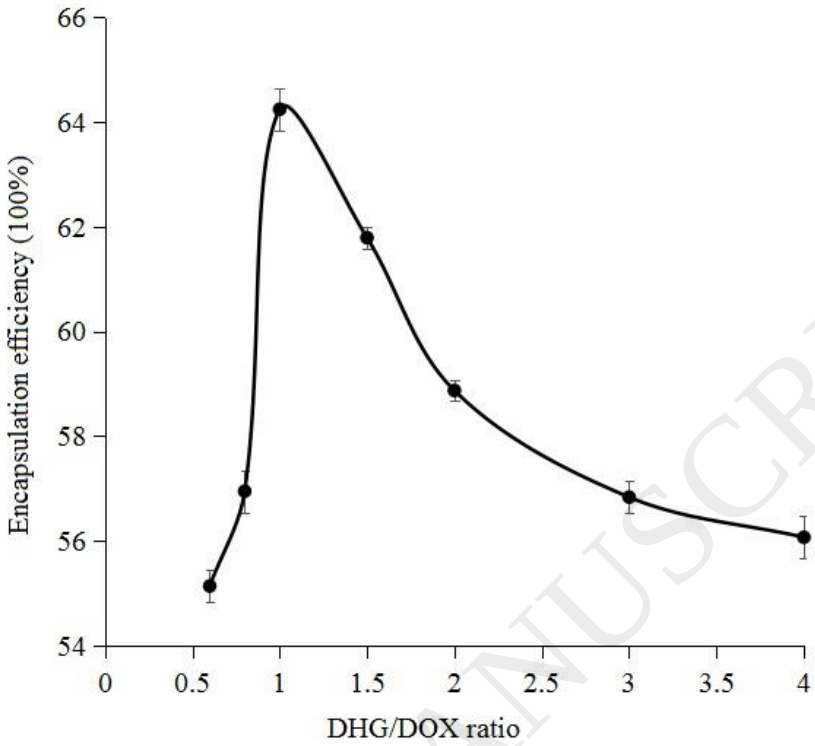

Fig. 1 Effect of depolymerized holothurian glycosaminoglycans/doxorubicin (DHG/DOX) ratio on encapsulation efficiency of DHG-DOX nanocomplexes.

3.3 The surface morphology of nanocomplexes

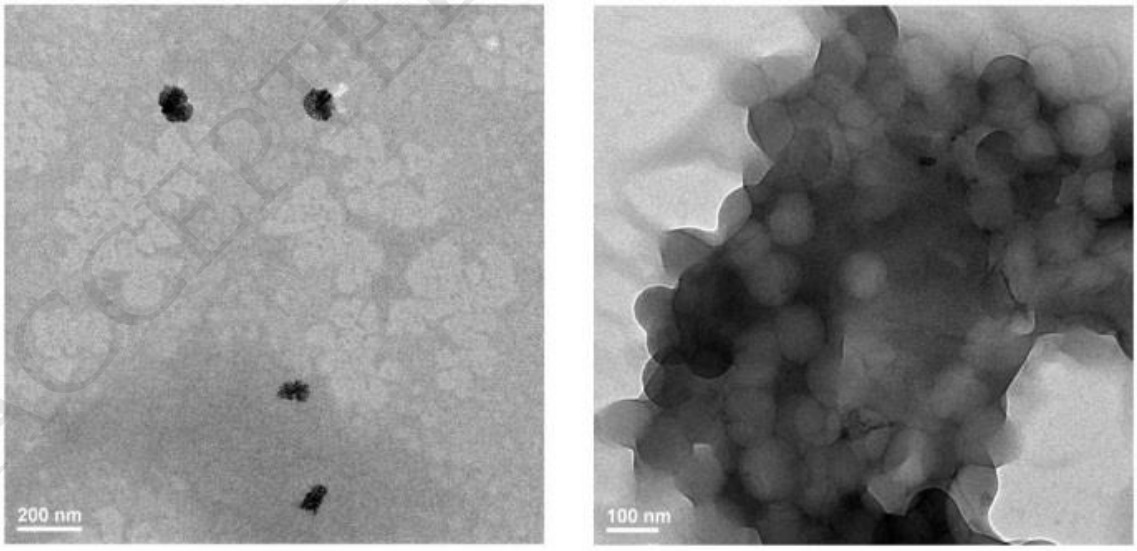

Fig. 2 Transmission electron microscopy image of DHG-DOX nanocomplexes (DOX: 0.5mg/mL, DHG/DOX: 1.0)

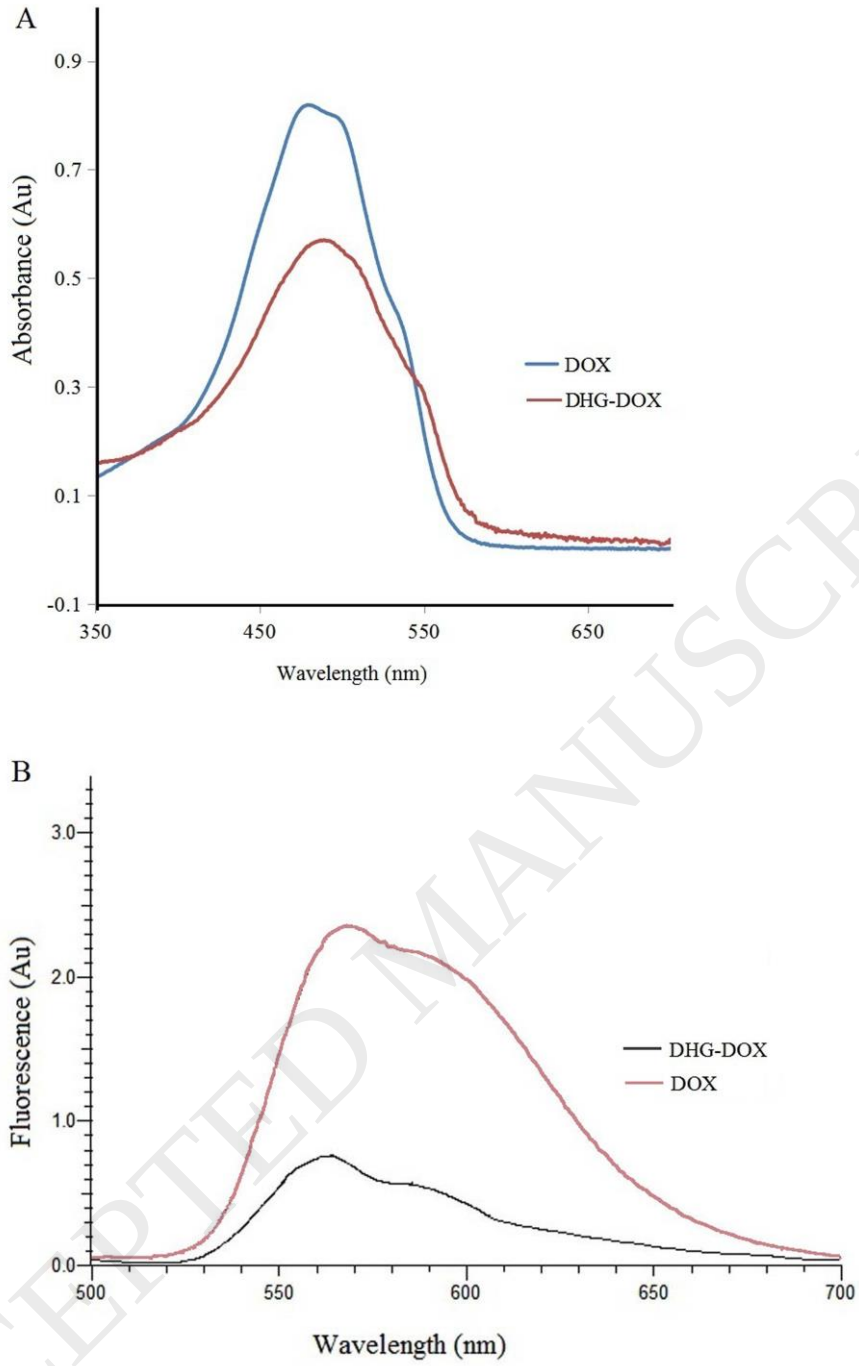

Fig. 3 UV-visible spectrum (A) and fluorescence spectrum (B) of free DOX and DHG-DOX nanocomplexes (DOX: 0.5mg/mL, DHG/DOX: 1.0)

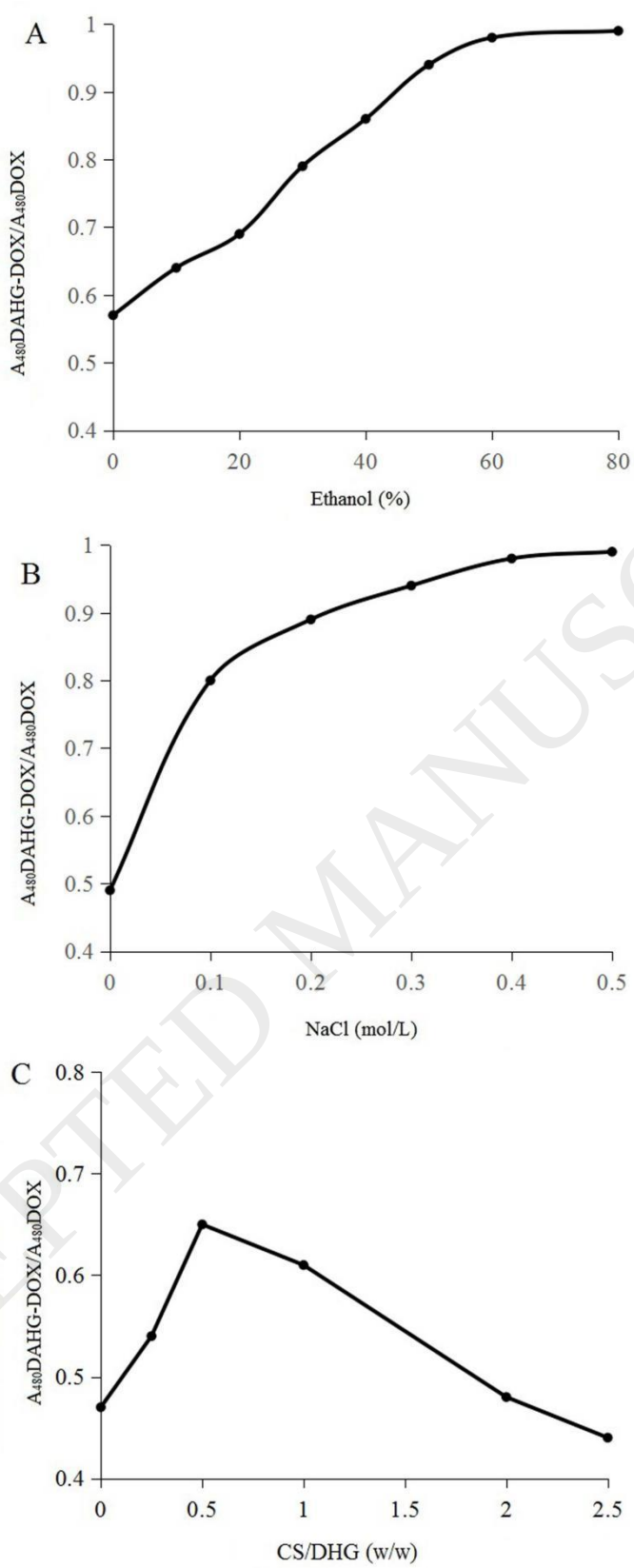

Fig. 4 Effect of ethanol concentration (A), NaCl concentration (B) and polycationic chitosan (CS) on the DHG-DOX nanocomplexes (DOX: 0.5mg/mL, DHG/DOX: 1.0)

3.6 In vitro release profiles of DHG-DOX nanocomplexes

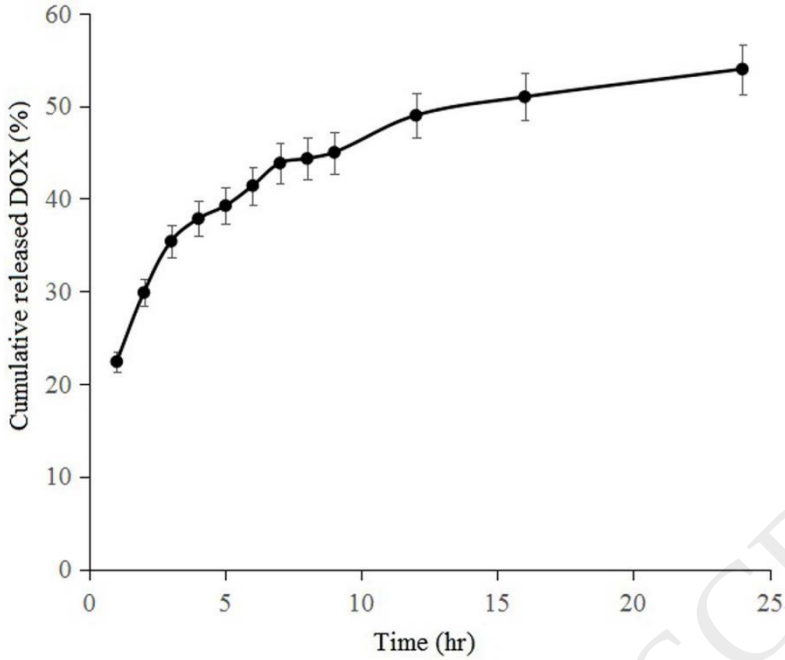

Fig. 5 In vitro cumulative release of doxorubicin (DOX) from DHG-DOX nanocomplexes (DOX: 0.5mg/mL, DHG/DOX: 1.0) (n=3), 37 °C.

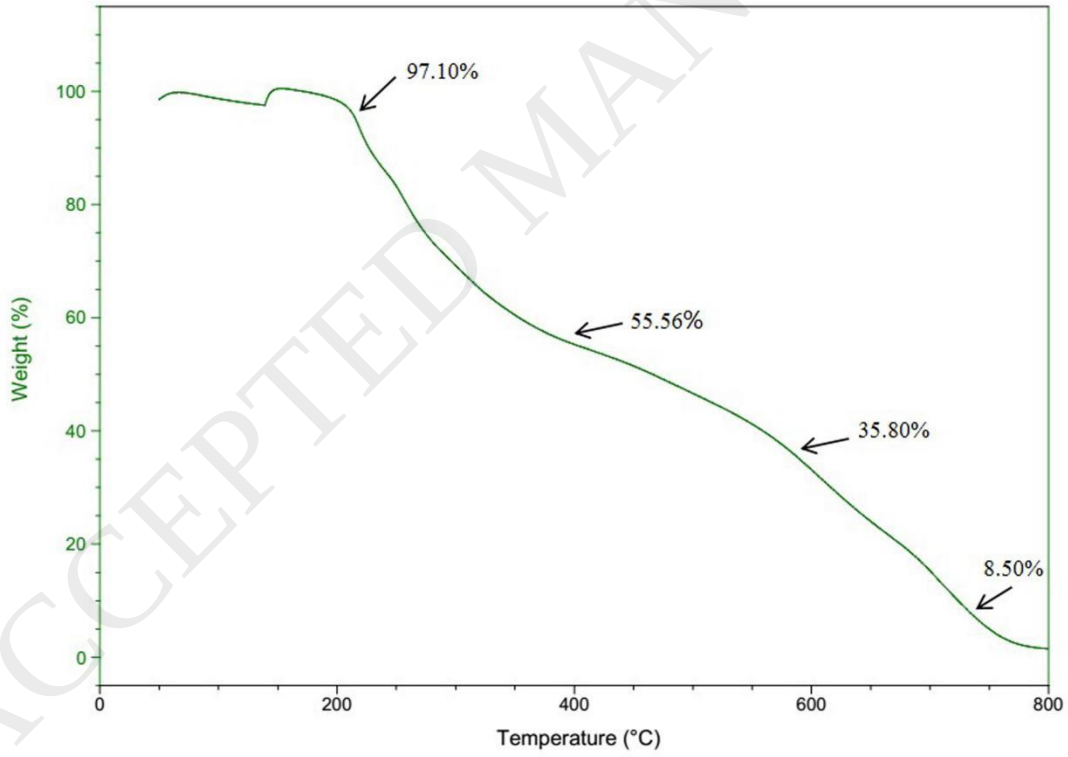

Fig. 6 Thermogravimetric analysis (TGA) of DHG-DOX nanocomplexes. (DOX: 0.5mg/mL, DHG/DOX: 1.0).

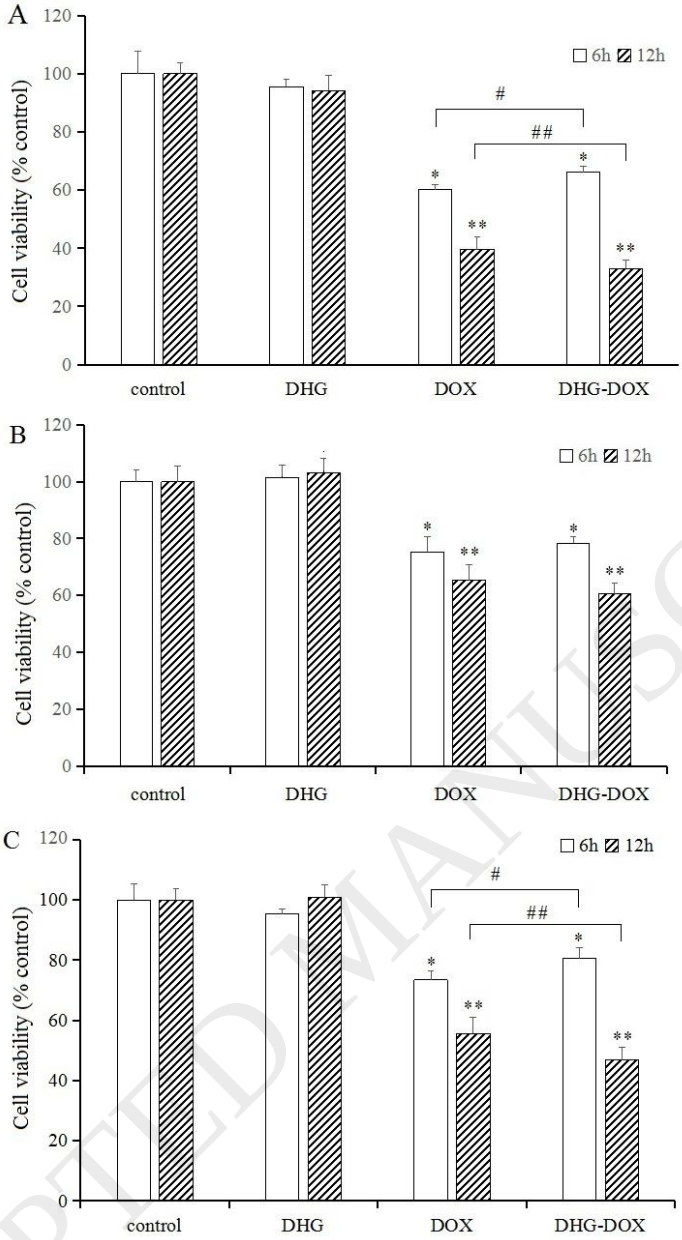

Fig. 7 Cell viability of HepG-2 (A), MCF-7 (B) and A549 (C) cells after incubation for 6h and 12h with free DOX·HCl (25 μg/mL) and the DOX loaded DHG-DOX nanocomplexes (DOX: 25 μg/mL, DHG/DOX: 1.0). (Mean ± S.D., n=6; *, vs control at 6h, $p < 0.01$; *, vs control at 12h, $p < 0.01$; #, ##, $p < 0.05$).

Scheme

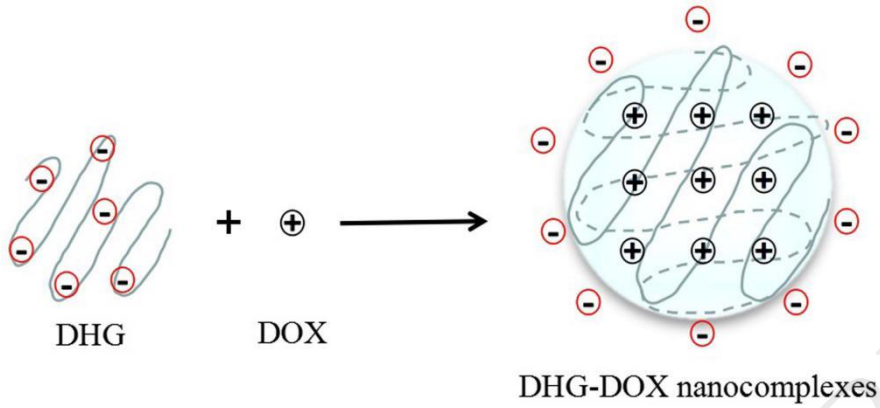

Scheme 1. Schematic illustration of the complexation of DHG and DOX.

Tables

Table 1. Size and zeta potential value of DHG-DOX nanocomplex at different ratio

DHG/DOX (w/w)	Diameter/nm	PDI	Zeta potential value/mV
0.6:1	353.5±24.1	0.622	-34.5±2.6
1:1	265.4±16.2	0.584	-46.3±1.5
2:1	219.5±33.4	0.560	-53.8±2.0